Inorg. Chem. **2008**, *47*, 793–804

Inorganic Chemistry
Article

Colorimetric Fluoride Ion Sensing by Polyborylated Ferrocenes: Structural Influences on Thermodynamics and Kinetics

Joanna K. Day,[†,‡] Christopher Bresner,[†,‡] Natalie D. Coombs,[†,‡] Ian A. Fallis,*[‡] Li-Ling Ooi,[‡] and Simon Aldridge*[†]

Inorganic Chemistry, University of Oxford, South Parks Road, Oxford, U.K., OX1 3QR, and
School of Chemistry, Cardiff University, Main Building, Park Place, Cardiff, U.K., CF10 3AT

Received July 26, 2007

The thermodynamic factors underlying the use of ferroceneboronic esters as electrochemical or colorimetric fluoride ion sensors have been investigated through the synthesis of a range of systematically related derivatives differing in the number/nature of the boronic ester substituents and in the nature of ancillary ligands. Thus, if the shift in electrochemical potential associated with the conversion of one (or more) boronic ester group(s) to anionic boronate(s) on fluoride binding is sufficient to allow oxidation of the resulting host/guest complex by dioxygen, colorimetric sensing is possible. In practice, while monofunctional systems of the type CpFe[η^5-$C_5H_4B(OR)_2$] offer *selectivity* in fluoride binding, electrochemical shifts in chloroform solution are insufficient to allow for a colorimetric response. Two chemical modification strategies have been shown to be successful in realizing a colorimetric sensor: (i) the use of the more strongly electron-donating Cp* ancillary ligand (which shifts the oxidation potential of *both* the free receptor and the resulting fluoride adduct cathodically by ca. –400 mV) and (ii) receptors featuring two or more binding sites and consequently a larger fluoride-induced electrochemical shift. Thus, in the case of [η^5-$C_5H_4B(OR)_2]_2$Fe [$(OR)_2$ = OC(H)PhC(H)PhO, **2**^{s}], the binding of 2 equiv of fluoride gives an electrochemical shift (in chloroform) of –960 mV (cf. –530 mV for the corresponding monofunctional analogue, **1**^{s}). Related tris- and tetrakis-functionalized systems are also shown to be oxidized as the bis(fluoride) adducts, presumably because of fast oxidation kinetics, relative to the rate of the (electrostatically unfavorable) binding of a third equivalent of fluoride. Furthermore, the *rate* of sensor response (as measured by UV/vis spectroscopy) is found to be strongly enhanced by the presence of pendant (uncomplexed) three-coordinate boronic ester functions (e.g., a rate enhancement of 1–2 orders of magnitude for **3**^{s}/**4**^{s} with respect to **2**^{s}) and/or delocalized aromatic substituents.

Introduction

Anion and neutral molecule recognition has been the subject of considerable recent research interest, reflecting not only relevance to key biological systems, but also potential applications in sensors and in separation technologies.[1] Within this field, fluoride detection is a topical area with considerable significance to health and environmental issues; gaseous sources such as hydrogen fluoride, for example, are known to be liberated in the hydrolysis of fluorinated G-type chemical warfare agents (CWAs), while domestically, the monitoring of fluoride levels in drinking water is of some importance.[2] Thus, a number of receptor systems have been reported capable of the selective binding of fluoride; in addition to well-developed host/guest strategies based on electrostatic and/or hydrogen bonding interactions,[1] a number of alternative receptors based on Lewis acidic binding domains have been reported.[3−6] The relative strength of fluoride binding (cf. other anions) by three-coordinate boron, for example, has been exploited in the development of systems which will selectively recognize fluoride in solution.[3,4] In terms of sensor development, analyte-specific binding needs to be coupled with an observable reporter response accompanying formation of the target host−guest complex. Fluorescent or electrochemical reporting of the binding event have been exploited to great effect, and a number of convenient colorimetric systems for the detection of fluoride have also been described.[7]

In preliminary work on boronic esters containing a ferrocene backbone, we reported a bifunctional Lewis acid [η^5-$C_5H_4B(OR)_2]_2$Fe [$(OR)_2$ = OC(H)PhC(H)PhO, **2**^{s}] which

---

* To whom correspondence should be addressed. E-mail: simon.aldridge@chem.ox.ac.uk (S.A.); fallis@cardiff.ac.uk (I.A.F.).
[†] University of Oxford.
[‡] Cardiff University.

10.1021/ic701494p CCC: $40.75

can act as a colorimetric sensor for fluoride.[8] With a view to developing this prototype system toward sensors offering improved *kinetics* and/or *sensitivity* of response, we have targeted a better understanding of key thermodynamic and kinetic factors underlying the oxidation-based colorimetric response. Ultimately a better understanding of these important issues should enable tuning of sensor properties by simple chemical modification. Thus, the effects of the number/nature of boronic ester substituents and of ancillary ligands on the efficacy and rate of the colorimetric response have been systematically evaluated and are reported herein. In addition, parallel studies have targeted the use of redox-matched high extinction coefficient dyes in order to improve the *sensitivity* of fluoride detection to sub-micromolar levels.[9]

Experimental Section

i. General Considerations. Manipulations of air-sensitive reagents were carried out under a nitrogen or argon atmosphere using standard Schlenk line or dry box techniques. Solvents were predried over sodium wire (hexanes, toluene, benzene, THF) or molecular sieves (acetonitrile, chloroform, dichloromethane) and purged with nitrogen prior to distillation from the appropriate drying agent (hexanes and THF, potassium; toluene and benzene, sodium; acetonitrile and dichloromethane, CaH_2). [D_6]Benzene, [D_8]toluene, [D]chloroform, and [D_2]dichloromethane (Goss) were degassed and dried over potassium ([D_6]benzene, [D_8]toluene) or molecular sieves ([D]chloroform, [D_2]dichloromethane) prior to use. Triethylamine

---

(1) For recent reviews of anion binding, see, for example: (a) de Silva, A. P.; Gunaratne, H. Q. N.; Gunnlaugsson, T.; Huxley, A. J. M.; McCoy, C. P.; Rademacher, J. T.; Rice, T. E. *Chem. Rev*. **1997**, *97*, 1515. (b) Schmidtchen, F. P.; Berger, M. *Chem. Rev*. **1997**, *97*, 1609. (c) Gale, P.A.; Sessler, J.A.; Kral, V. *Chem. Commun.* **1998**, 1. (d) Beer, P. D.; Gale, P. A. *Angew. Chem., Int. Ed*. **2001**, *40*, 486. (e) Lavigne, J. J.; Anslyn, E. V. *Angew. Chem., Int. Ed*. **2001**, *40*, 3118. (f) Martínez-Máñez, R.; Sancernón, F. *Chem. Rev*. **2003**, *103*, 4419. (g) Best, M. D.; Tobey, S. L.; Anslyn, E. V. *Coord. Chem. Rev*. **2003**, *240*, 3. (h) Sessler, J. A.; Camiolo, S.; Gale, P. A. *Coord. Chem. Rev*. **2003**, *240*, 17. (i) Llinares, J. M.; Powell, D.; Bowman-James, K. *Coord. Chem. Rev*. **2003**, *240*, 57. (j) Loeb, S.; Bondy, C. R. *Coord. Chem. Rev*. **2003**, *240*, 77. (k) Choi, K.; Hamilton, A. D. *Coord. Chem. Rev*. **2003**, *240*, 101. (l) Beer, P. D.; Hayes, E. J. *Coord. Chem. Rev*. **2003**, *240*, 167. (m) O'Neill, E. J.; Smith, B. D. *Coord. Chem. Rev*. **2006**, *250*, 3068. (n) Filby, M. H.; Steed, J. W. *Coord. Chem. Rev*. **2006**, *250*, 3200. (o) Gale, P. A.; Quesada, R. *Coord. Chem. Rev*. **2006**, *250*, 3219.

(2) (a) Yang, Y.-C.; Baker, J. A.; Ward, J. R. *Chem. Rev*. **1992**, *92*, 1729. (b) Sohn, H.; Létant, S.; Sailor, M. J.; Trogler, W. C. *J. Am. Chem. Soc*. **2000**, *122*, 5399. (c) Bresner, C.; Aldridge, S.; Fallis, I. A.; Jones, C.; Ooi, L.-L. *Angew. Chem., Int. Ed.* **2005**, *44*, 3606. (d) Colquhoun, J. *Perspect. Biol. Med.* **1997**, *41*, 29. (e) Carton, R. J. *Fluoride* **2006**, *39*, 163.

(3) For previous examples of fluoride binding by boronic acid/esters see, for example: (a) Dusemund, C.; Sandanayake, K.R.A.S.; Shinkai, S. *J. Chem. Soc., Chem. Commun.* **1995**, 333. (b) Yamamoto, H.; Ori, A.; Ueda, K.; Dusemund, C.; Shinkai, S. *J. Chem. Soc., Chem. Commun.* **1996**, 407. (c) Cooper, C.R.; Spencer, N.; James, T.D. *J. Chem. Soc., Chem. Commun.* **1998**, 1365. (d) Yuchi, A.; Tatebe, A.; Kani, S.; James, T. D. *Bull. Chem. Soc. Jpn.* **2001**, *74*, 509. (e) Nicolas, M.; Fabre, B.; Simonet, J. *Electrochim. Acta* **2001**, *46*, 1179. (f) Fabre, B.; Lehmann, U.; Schlüter, A. D. *Electrochim. Acta.* **2001**, *46*, 2855. (g) DiCesare, N.; Lakowicz, J. R. *Anal. Biochem.* **2002**, *301*, 111. (h) Arimori, S.; Davidson, M.G.; Fyles, T.M.; Hibbert, T.G.; James, T.D.; Kociok-Köhn, G.I. *Chem. Commun.* **2004**, 1640. (i) Ramachandram, B.; Lakowicz, J.; Geddes, C. D. *Curr. Anal. Chem.* **2005**, *1*, 157. (j) Swamy, K. M. K.; Lee, Y. J.; Lee, H. N.; Chun, J.; Kim, Y.; Kim, S.-J.; Yoon, J. *J. Org. Chem.* **2006**, *71*, 8626.

(4) For fluoride binding by other three-coordinate boron-containing systems see, for example: (a) Yamaguchi, S.; Akiyama, S.; Tamao, K. *J. Am. Chem. Soc.* **2001**, *123*, 11372. (b) Yamaguchi, S.; Shirasaka, T.; Akiyama, S.; Tamao, K. *J. Am. Chem. Soc.* **2002**, *124*, 8816. (c) Miyata, M.; Chujo, Y. *Polym. J.* **2002**, *34*, 967. (d) Kubo, Y.; Yamamoto, M.; Ikeda, M.; Takeuchi, M.; Shinkai, S.; Tamao, K. *Angew. Chem., Int. Ed.* **2003**, *42*, 2036. (e) Solé, S.; Gabbaï, F.P. *Chem. Commun.* **2004**, 1284. (f) Herberich, G.E.; Englert, U.; Fischer, A.; Wiebelhaus, D. *Eur. J. Inorg. Chem.* **2004**, 4011. (g) Liu, Z. Q.; Shi, M.; Li, F. Y.; Fang, Q.; Chen, Z. H.; Yi, T.; Chuang, C. H. *Org. Lett.* **2005**, *7*, 5481. (h) Melaïmi, M.; Gabbaï, F. P. *J. Am. Chem. Soc.* **2005**, *127*, 5318. (i) Agou, T.; Kobayashi, J.; Kawashima, T. *Org. Lett.* **2005**, *7*, 4373. (j) Parab, K.; Venkatasubbaiah, K.; Jäkle, F. *J. Am. Chem. Soc.* **2006**, *128*, 12879. (k) Chiu, C.-W.; Gabbaï, F. P. *J. Am. Chem. Soc.* **2006**, *128*, 14248. (l) Agou, T.; Kobayashi, J.; Kawashima, T. *Inorg. Chem.* **2006**, *45*, 9137. (m) Sakuda, E.; Funahashi, A.; Kitamura, N. *Inorg. Chem.* **2006**, *45*, 10670. (n) Liu, X. Y.; Bai, D. R.; Wang, S. *Angew. Chem., Int. Ed.* **2006**, *45*, 5475. (o) Lee, M.H.; Agou, T.; Kobayashi, J.; Kawashima, T.; Gabbaï, F.P. *Chem. Commun.* **2007**, 1133. (p) Sun, Y.; Ross, N.; Zhao, S. B.; Huszarik, K.; Jia, W. L.; Wang, R. Y.; Macartney, D.; Wang, S. *J. Am. Chem. Soc.* **2007**, *129*, 7510. (q) Cui, Y.; Lu, Z.-H.; Wang, S. *Dalton Trans.* **2007**, 2634.

(5) For bidentate boron-centered Lewis acids see, for example: (a) Katz, H. E. *J. Am. Chem. Soc*. **1985**, *107*, 1420. (b) Katz, H. E. *J. Org. Chem*. **1985**, *50*, 5027. (c) Jia, L.; Yang, X.; Stern, C.; Marks, T. J. *Organometallics* **1994**, *13*, 3755. (d) Köhler, K.; Piers, W. E.; Sin, X.; Feng, Y.; Bravakis, A. M.; Jarvis, A. P.; Collins, S.; Clegg, W.; Yap, G. P. A.; Marder, T. B. *Organometallics* **1998**, *17*, 3557. (e) Williams, V. C.; Piers, W. E.; Clegg, W.; Elsegood, M. R. J.; Collins, S.; Marder, T. B. *J. Am. Chem. Soc*. **1999**, *121*, 3244. (f) Williams, V. C.; Dai, C.; Li, Z.; Collins, S.; Piers, W. E.; Clegg, W.; Elsegood, M. R. J.; Marder, T. B. *Angew. Chem., Int. Ed*. **1999**, *38*, 3695. (g) Metz, M. V.; Schwartz, D. J.; Stern, C. L.; Nickias, P. N.; Marks, T. J. *Angew. Chem., Int. Ed*. **2000**, *39*, 1312. (h) Williams, V. C.; Irvine, G. J.; Piers, W. E.; Li, Z. M.; Collins, S.; Clegg, W.; Elsegood, M. R. J.; Marder, T. B. *Organometallics* **2000**, *19*, 1619. (i) Piers, W.E.; Irvine, G.; Williams, V.C. *Eur. J. Inorg. Chem.* **2000**, 2131. (j) Hoefelmeyer, J. D.; Schulte, M.; Tschinkl, M.; Gabbaï, F. P. *Coord. Chem. Rev*. **2002**, *235*, 93. (k) Henderson, L. D.; Piers, W. E.; Irvine, G. J.; McDonald, R. *Organometallics* **2002**, *21*, 340. (l) Metz, M. V.; Schwartz, D. J.; Stern, C. L.; Marks, T. J.; Nickias, P. N. *Organometallics* **2002**, *21*, 4159. (m) Emslie, D. J. M.; Piers, W. E.; Parvez, M. *Angew. Chem., Int. Ed*. **2003**, *42*, 1252. (n) Gabbaï, F. P. *Angew. Chem., Int Ed*. **2003**, *42*, 2218. (o) Lewis, S. P.; Taylor, N. J.; Piers, W. E.; Collins, S. *J. Am. Chem. Soc*. **2003**, *125*, 14686. (p) Ghesner, I.; Piers, W. E.; Parvez, M.; McDonald, R. *Organometallics* **2004**, *23*, 3085. (q) Morrison, D. J.; Piers, W. E.; Parvez, M. *Synlett.* **2004**, *13*, 2429. (r) Piers, W. E. *Adv. Organomet. Chem.* **2005**, *52*, 1. (s) Melaimi, M.; Gabbaï, F. P. *Adv. Organomet. Chem.* **2005**, *52*, 61. (t) Scheibitz, M.; Heilmann, J.B.; Winter, R.F.; Bolte, M.; Bats, J.W.; Wagner, M. *Dalton Trans.* **2005**, 159. (u) Scheibitz, M.; Bolte, M.; Bats, J. W.; Lerner, H.-W.; Nowik, I.; Herber, R. H.; Krapp, A.; Lein, M.; Holthausen, M.; Wagner, M. *Chem. Eur. J.* **2005**, *11*, 584. (v) Venkatasubbaiah, K.; Zakharov, L. N.; Kassel, W. S.; Rheingold, A. L.; Jäkle, F. *Angew. Chem., Int. Ed.* **2005**, *44*, 5429. (w) Gabbaï, F. P. *A.C.S. Symp. Ser*. **2006**, *917*, 208. (x) Chase, P. A.; Henderson, L. D.; Piers, W. E.; Parvez, M.; Clegg, W.; Elsegood, M. R. J. *Organometallics* **2006**, *25*, 349. (y) Venkatasubbaiah, K.; Nowil, I.; Herber, R. H.; Jäkle, F. *Chem. Commun.* **2007**, 2154.

(6) For examples of Lewis base binding by non-boron-containing Lewis acids see, for example: (a) Tamao, K.; Hayashi, T.; Ito, Y. *J. Organomet. Chem.* **1996**, *506*, 85 [Si]. (b) Wedge, T. J.; Hawthorne, M. F. *Coord. Chem. Rev*. **2003**, *240*, 111 [Hg]. (c) Gabbaï, F.P.; Schier, A.; Riede, J.; Hynes, M. J. *Chem. Commun.* 1998, 897 [In]. (d) Uhl, W.; Hannemann, F.; Saak, W.; Wartchow, R. *Eur. J. Inorg. Chem.* **1998**, 921 [Al]. (e) Hoefelmeyer, J. D.; Gabbaï, F. P. *Chem. Commun.* **2003**, 712 [Ga, Sn]. (f) Haneline, M. R.; Gabbaï, F. P. *Angew. Chem., Int. Ed.* **2004**, *43*, 5471 [Hg]. (g) Chaniotakis, N.; Jurkschat, K.; Mueller, D.; Perdikaki, K.; Reeske, G. *Eur. J. Inorg. Chem.* **2004**, 2283 [Sn]. (h) Boshra, R.; Sundararaman, A.; Zakharov, L. N.; Incarvito, C. D.; Rheingold, A. L.; Jäkle, F. *Chem. Eur. J.* **2005**, *11*, 2810 [Sn]. (i) Badr, I. H. A; Meyerhoff, M. E. *J. Am. Chem. Soc.* **2005**, *127*, 5318 [Al].

(7) For recent reviews on approaches to fluorescent or colorimetric reporting, see for example: (a) Martínez-Máñez, R.; Sancerón, F. *Coord. Chem. Rev*. **2006**, *250*, 3081. (b) Gunnlaugsson, T.; Glynn, M.; Tocci, (née Hussey), G. M.; Kruger, P. E.; Pfeffer, F. M. *Coord. Chem. Rev*. **2006**, *250*, 3094. (c) Nguten, B. T.; Anslyn, E. V. *Coord. Chem. Rev*. **2006**, *250*, 3118.

(8) Aldridge, S.; Bresner, C.; Fallis, I. A.; Coles, S. J.; Hursthouse, M. B. *Chem. Commun.* **2002**, 740.

(9) Bresner, C.; Day, J. K.; Fallis, I. A.; Aldridge, S. in preparation.

Scheme 1. Syntheses of Ferrocene-Based Lewis Acids Containing One, Two, or Four Pendant Boronic Ester Functions[a]

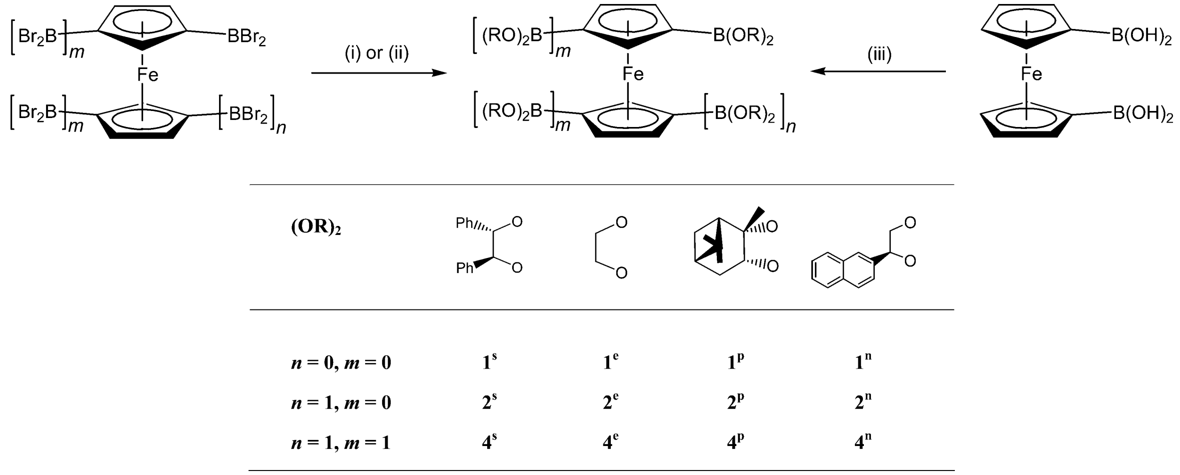

[a] Reagents and conditions: (i) diol dilithiate (1.0, 2.0, or 4.0 equiv, respectively, for mono-, bis-, and tetrakis-functionalized systems; prepared in situ from diol and 2.0 equiv of ^{n}BuLi), toluene, 20 °C, 24 h, 37−64%; (ii) diol, triethylamine (1.0, 2.0, or 4.0 equiv of each), toluene, 20 °C, 24 h, ca. 50%; (iii) $\mathbf{2^{n}}$, diol (2 equiv), acetone, 75 °C (sealed high-pressure tube), 24 h, 18%.

(Alfa) was dried over sodium wire before use. *n*-Butyllithium (Acros), ethane-1,2-diol, tetra-*n*-butylammonium fluoride, potassium fluoride, and 18-crown-6 (all Aldrich) were used as supplied. $\mathbf{1^{s}}$, $\mathbf{2^{s}}$, $\mathbf{1^{e}}$, and $\mathbf{2^{e}}$ were synthesized as reported previously.[8−10] Dibromoboryl derivatives of ferrocene and alkylferrocenes were prepared by minor modification of established procedures.[11,12] *R*,*R*-Hydrobenzoin and *S*-(2-napthyl)ethane-1,2-diol were prepared by asymmetric dihydroxylation of the corresponding alkene using literature protocols.[13]

NMR spectra were measured on a Bruker AM-400 or JEOL 300 Eclipse Plus FT-NMR spectrometer. Residual signals of solvent were used as reference for ^{1}H and ^{13}C NMR; ^{11}B and ^{19}F NMR spectra were referenced with respect to $Et_2O{\cdot}BF_3$ and $CFCl_3$, respectively. The ^{13}C signals due to boron-bound C_5H_4 carbons were typically broad or not observed. Infrared spectra were measured for each compound pressed into a disk with an excess of dried KBr or as a solution in an appropriate solvent on a Nicolet 500 FT-IR spectrometer. Mass spectra were measured by the EPSRC National Mass Spectrometry Service Centre, University of Wales, Swansea, or by the departmental service. Perfluorotributylamine was used as a standard for high-resolution measurements. Satisfactory analyses were obtained for new compounds (see Supporting Information). Abbreviations: b = broad, s = singlet, d = doublet, t = triplet, q = quintet, m = multiplet. Abbreviations used in chemical numbering ($\mathbf{1^{s}}$, $\mathbf{2^{p}}$, etc.): s = *R*,*R*-hydrobenzoin diolate (stibene diolate) boronic ester backbone; e = 1,2-ethanediolate; p = 1*S*,2*S*,3*R*,5*S*-pinanediolate, n = *S*-(2-napthyl)ethane-1,2-diolate.

ii. Syntheses. Synthesis of $\mathbf{1^{p}}$. $\mathbf{1^{p}}$ was synthesized from (dibromoboryl)ferrocene via route (i) outlined in Scheme 1. Similar procedures were followed for the syntheses of $\mathbf{2^{n}}$, $\mathbf{3^{s}}$, $\mathbf{3^{p}}$, $\mathbf{4^{s}}$, $\mathbf{4^{p}}$, and $\mathbf{4^{n}}$ from 1,1′-bis(dibromoboryl)ferrocene, 1′,3,3′-tris(dibromoboryl)ethylferrocene, and 1,1′,3,3′-tetrakis(dibromoboryl)ferrocene, with the caveat that 2, 3, or 4 equiv, respectively, of the diol reagent were employed for the syntheses of bis-, tris-, and tetrakis-functionalized ferroceneboronic esters (Schemes 2 and 3). In addition, $\mathbf{1^{*s}}$ and $\mathbf{2^{*s}}$ were synthesized from 1′-(dibromoboryl)-1,2,3,4,5-pentamethylferrocene and 1′,3′-bis(dibromoboryl)-1,2,3,4,5-pentamethylferrocene, respectively, by an analogous method (Scheme 3). For $\mathbf{1^{p}}$: To a solution of 1*S*,2*S*,3*R*,5*S*-2,3-pinanediol (0.46 g, 2.7 mmol) in toluene (ca. 25 cm^{3}) at −78 °C was added dropwise *n*-butyllithium (3.4 cm^{3} of a 1.6 M solution in hexanes, 2 equiv). The resulting slurry was warmed to room temperature and stirred for a further 2 h. A solution of dibromoborylferrocene (1 equiv) in toluene was then added at room temperature, and the reaction mixture stirred for 24 h. Filtration and removal of the toluene solvent in vacuo afforded an oily orange residue, which was extracted with hexanes or 40:60 petroleum ether and crystallized at −30 °C to yield $\mathbf{1^{p}}$ as an air-stable orange crystalline solid in ca. 40% yield. Single crystals were obtained by slow cooling of a concentrated acetonitrile solution from 40 °C to room temperature.

Scheme 2. Syntheses of Ethylferrocene-Based Lewis Acids Containing Three Pendant Boronic Ester Functions[a]

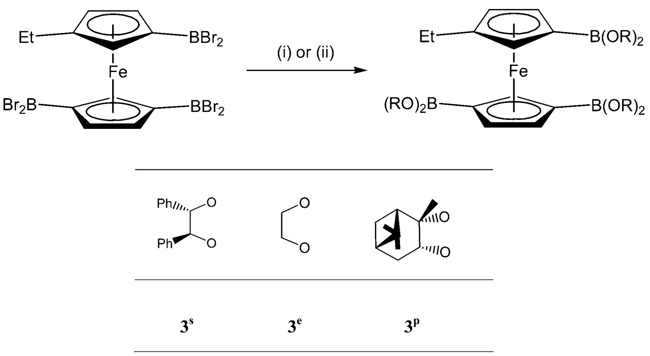

[a] Reagents and conditions: (i) diol dilithiate (3.0 equiv; prepared in situ from diol and 2.0 equiv of ^{n}BuLi), toluene, 20 °C, 24 h, 38−46%; (ii) diol, triethylamine (3.0 equiv of each), toluene, 20 °C, 24 h, ca.40%.

Spectroscopic Data for $\mathbf{1^{p}}$. ^{1}H NMR ([D]chloroform, 20 °C): δ 0.42 [s, 3H, H-8], 0.93 [s, 3H, H-9], 1.21 [s, 3H, H-10], 1.33 [d $J = 10$ Hz, 1H, H-6a], 1.55 [m, 1H, H-5], 1.89−2.08 [overlapping m, 4H, H-1, H-4a, H-4b, H-6b], 4.03 [s, 5H, C_5H_5], 4.10 [m, 2H, C_5H_4], 4.11 [d, 1H, H-3], 4.58 [d, 2H, C_5H_4]. ^{13}C NMR ([D]chloroform, 20 °C): δ 22.5, 25.5, 25.7, 27.9, 34.7, 36.8, 38.5, 50.4, 73.1, 76.7 [pinane backbone], 67.5 [C_5H_5], 70.9 [C_5H_4], 73.0 [C_5H_4]. ^{11}B NMR ([D]chloroform, 20 °C): δ 30.1. IR (KBr disk, cm^{-1}): ν 2930 md, 1501 md, 1482 s, 1382 s, 1324 s, 1261 md, 1189 w, 1130 s, 1034 md, 909 w, 816 s, 702 w, 688 md, 598 w. UV/vis

---

(10) Bresner, C.; Day, J. K.; Coombs, N. D.; Fallis, I. A.; Aldridge, S.; Coles, S. J.; Hursthouse, M. B. *Dalton Trans.* **2006**, 3660.

(11) (a) Appel, A.; Nöth, H.; Schmidt, M. *Chem. Ber.* **1995**, *128*, 621. (b) Appel, A.; Jäkle, F.; Priermeier, T.; Schmid, R.; Wagner, M. *Organometallics* **1996**, *15*, 1188.

(12) (a) Ma, K.; Scheibitz, M.; Scholz, S.; Wagner, M. *J. Organomet. Chem.* **2002**, *652*, 11. (b) U. Dörfler, Ph.D. thesis, University of Bayreuth, 1994.

(13) Sharpless, K. B. *Chem. Rev.* **1994**, *94*, 2483.

Scheme 3. Syntheses of Pentamethyferrocene-Based Lewis Acids Containing One or Two Pendant Boronic Ester Functions[a]

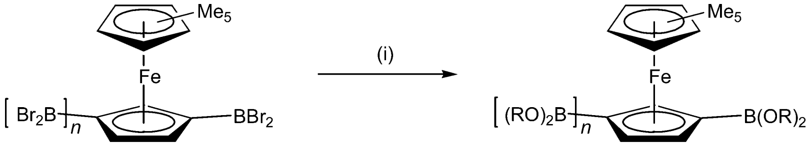

	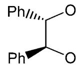
***n* = 0**	$\mathbf{1}^{*s}$
***n* = 1**	$\mathbf{2}^{*s}$

[a] Reagents and conditions: (i) diol dilithiate (1.0 or 2.0 equiv, respectively, for mono- and bis-functionalized systems; prepared in situ from diol and 2.0 equiv of ^{n}BuLi), toluene, 20 °C, 24 h, ca.60%.

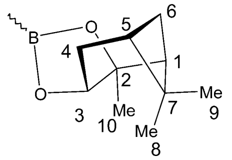

Figure 1. Numbering scheme for 1*S*,2*S*,3*R*,5*S*-pinane diolate substituents.

(chloroform): $\lambda_{\max} = 472$ nm, $\epsilon = 134$ mol^{-1} cm^{-1} dm^3. MS (EI): M$^+$ = 364.1 (100%), exact mass (calcd) *m*/*z* 364.1292, (obs.) 364.1290. (See Figure 1 for numbering scheme).[14]

Spectroscopic Data for 2^n. ^{1}H NMR ([D$_6$]benzene, 20 °C): δ 3.96 [m, 1H, CH$_2$ of chelate], 4.27 [m, 1H, CH$_2$ of chelate], 4.40 [m, 4H, C$_5$H$_4$], 4.87 [m, 4H, C$_5$H$_4$], 5.38 [m, 1H, CH of chelate], 7.23−7.26 [m, 6H, C$_{10}$H$_7$], 7.58−7.74 [m, 8H, C$_{10}$H$_7$]. ^{1}H NMR ([D]chloroform, 20 °C): δ 4.22 [m, 2H, CH$_2$ of chelate], 4.51 [m, 4H, C$_5$H$_4$], 4.59 [m, 4H, C$_5$H$_4$], 4.76 [m, 2H, CH$_2$ of chelate], 5.70 [m, 2H, CH of chelate], 7.46−7.49 [m, 6H, C$_{10}$H$_7$], 7.81−7.88 [m, 8H, C$_{10}$H$_7$]. ^{13}C NMR ([D$_6$]benzene, 20 °C): δ 72.9 [CH of C$_5$H$_4$], 73.2 [CH$_2$ of chelate], 75.0 [CH of C$_5$H$_4$], 75.3 [CH of C$_5$H$_4$], 78.9 [CH of chelate], 123.6, 124.1, 125.0, 126.0, 126.3, 128.7, 129.1 [aromatic CH], 133.4, 133.5, 138.9 [aromatic quaternary]. ^{11}B NMR ([D$_6$]benzene, 20 °C): δ 33.2. IR (KBr disk, cm^{-1}): ν 2956 w, 2895 w, 1579 w, 1488 st, 1473 st, 1378 md, 1322 md, 1292 w, 1132 st, 1046 w, 996 w, 825 w. UV/vis (chloroform): $\lambda_{\max}$ (ε) 447 nm, $\epsilon = 132$ mol^{-1} cm^{-1} dm^3. MS(EI): M$^+$ = 578 (18%), exact mass (calcd) *m*/*z* 578.1518, (obs) 578.1521. 45% yield after recrystallization from warm hexanes (air-stable orange crystalline solid).

Spectroscopic Data for 3^s. ^{1}H NMR ([D]chloroform, 20 °C): δ 1.08 [t *J* = Hz, 3H, CH$_3$ of Et], 2.38 [m, 2H, CH$_2$ of Et], 4.47, 4.50, 4.55, 4.63, 4.85, 5.01 [s, each 1H, CH of chelate], 5.13 [m, 2H, C$_5$H$_3$], 5.14 [m, 2H, C$_5$H$_3$], 5.22 [s, 1H, C$_5$H$_3$], 5.25[s, 1H, C$_5$H$_3$], 7.25−7.67 [m, 30H, aromatic CH]. ^{13}C NMR ([D]chloroform, 20 °C): δ 14.0, 21.1 [Et], 72.6, 73.6, 74.1, 77.7, 78.5, 81.0 [CH of C$_5$H$_3$], 85.6 (three closely spaced resonances at 85.57, 85.59, 85.62) [CH of chelate], 125.0, 125.2, 125.3, 127.0, 127.1, 127.2, 127.5, 127.6, 127.7 [aromatic CH], 138.7, 138.8, 139.3 [aromatic quaternary]. ^{11}B NMR ([D]chloroform, 20 °C): δ 34.1 (b). IR (KBr disk, cm^{-1}) ν 2923 s, 1463 s, 1376 s, 1274 s, 1209 md, 1078 w, 1059 md, 986 md, 844 w, 759 md, 697 s, 650 w, 611 w. UV/vis (chloroform): $\lambda_{\max} = 454$ nm, $\epsilon = 253$ mol^{-1} cm^{-1} dm^3. MS (EI): M$^+$ = 880 (100%), exact mass (calcd) *m*/*z* 880.2996, (obs) 880.2997. 46% yield after recrystallization from acetonitrile/water (air-stable orange crystalline solid).

Spectroscopic Data for 3^p. ^{1}H NMR ([D]chloroform, 20 °C): δ 0.82 [s, 9H, C-10], 1.09 [t *J* = 5 Hz, 3H, CH$_3$ of Et], 1.24 [s, 9H, C-9], 1.20 [m, 3H], 1.41 [overlapping singlets, 9H, C-8], 1.87 [m, 6H], 2.04 [m, 3H], 2.31 [m, 3H], 2.33 [m, 5H], 4.15−4.52 (overlapping m, 9H, C$_5$H$_3$ and H-3]. ^{13}C NMR ([D]chloroform, 20 °C): δ 12.9, 21.9 [Et], 24.1, 26.7 (three overlapping signals), 27.2, 29.0, 35.7 (three overlapping signals), 38.2, 39.7, 51.4 (three overlapping signals), 77.8 (three overlapping signals), 85.6 (three overlapping signals) [pinane backbones], 73.4, 77.4, 77.7, 78.2, 81.9, 82.5 [CH of C$_5$H$_3$]. ^{11}B NMR ([D]chloroform, 20 °C): δ 32.8 (b). IR (KBr disk, cm^{-1}): ν 2923 s, 1716 w, 1462 s, 1375 s, 1304 md, 1233 md, 1122 md, 1078 md, 1061 w, 1025 w, 989 w, 937 w, 722 md. UV/vis (chloroform): $\lambda_{\max} = 454$ nm, $\epsilon = 218$ mol^{-1} cm^{-1} dm^3. MS (EI): M$^+$ = 754 (100%), exact mass (calcd) *m*/*z* 754.4044, (obs) 754. 4045. 38% yield after recrystallization from hexanes (air-stable orange solid). (See Figure 1 for numbering scheme).

Spectroscopic Data for 4^s: ^{1}H NMR ([D$_8$]toluene, 20 °C): δ 5.20 [m, 2H, C$_5$H$_3$], 5.23 [s, 4H, CH of chelate], 5.30 [m, 2H, C$_5$H$_3$], 5.34 [s, 4H, CH of chelate], 5.64 [s, 2H, C$_5$H$_3$], 7.01−7.24 [m, 40H, aromatic CH]. ^{13}C NMR ([D$_6$]benzene, 20 °C): δ 81.4, 81.8, 84.1 [C$_5$H$_3$], 88.4, 88.5 [CH of chelate], 127.7, 128.1, 129.8, 129.9, 138.6 (2 overlapping signals) [aromatic CH], 146.3, 146.5 [aromatic quaternary]. ^{11}B NMR ([D$_6$]benzene, 20 °C): δ 33.2 (b). IR (KBr disk, cm^{-1}): ν 3033 w, 1605 w, 1496 s, 1276 s, 1213 md, 1192 md, 1146 w, 1061 s, 988 s, 802 w, 760 md, 698 s, 538 md. UV/vis (chloroform): $\lambda_{\max} = 472$ nm, $\epsilon = 667$ mol^{-1} cm^{-1} dm^3. MS (EI): M$^+$ = 1074 (100%), exact mass (calcd) *m*/*z* 1074.3535, (obs) 1074.3546. 38% yield after recrystallization from toluene/hexanes (air-stable orange crystalline solid).

Spectroscopic Data for 4^p. ^{1}H NMR ([D]chloroform, 20 °C): δ 0.80 [s, 12H, H-10], 1.24 [s, 12H, H-9], 1.42 [s, 12H, H-8], 1.88 [overlapping m, 12H], 2.02 [t *J* = 5 Hz, 4H], 2.16 [m, 4H], 2.29 [m, 4H], 4.30 [t *J* = 7 Hz, 4H, H-3], 4.50 [m, 4H, C$_5$H$_3$], 4.56 [m, 2H, C$_5$H$_3$]. ^{13}C NMR ([D]chloroform, 20 °C): δ 23.8, 26.9, 29.1, 35.8, 37.9, 39.7, 51.6, 51.7,81.8, 85.6 [pinane backbone], 78.0 [C$_5$H$_5$], 78.2 [C$_5$H$_3$], 79.0 [C$_5$H$_3$]. ^{11}B NMR ([D]chloroform, 20 °C) δ 32.3 (b). IR (KBr disk, cm^{-1}): ν 3434 w, 2913 s, 2868 md, 2358 w, 1491 s, 1397 md, 1305 s, 1224 md, 1148 w, 1062 s, 988 w, 922 md, 692 s, 539 md. UV/vis (chloroform): $\lambda_{\max} = 472$ nm, $\epsilon = 203$ mol^{-1} cm^{-1} dm^3. MS (EI): M$^+$ = 898 (100%), exact mass (calcd) *m*/*z* 898.4787, (obs) 898.4796. 47% yield after

---

(14) Mass spectrometric data for compound $\mathbf{1}^p$ have been reported previously: Gamoh, K.; Ketuly, K. A.; Cole, W. J.; Brooks, C. J. W.; Anderson, R. A. *Anal. Sci.* **1994**, *10*, 705.

recrystallization from acetonitrile (air-stable orange crystalline solid). (See Figure 1 for numbering scheme).

Spectroscopic Data for 4^n. ^{1}H NMR ([D]chloroform, 20 °C): δ 4.13 [overlapping m, 4H, CH_2 of chelate], 4.42 [m, 2H, CH of chelate], 4.65 [m, 2H, CH of chelate], 4.74 [d, 2H, C_5H_3], 4.80 [d, 2H, C_5H_3], 4.95 [s, 2H, C_5H_3], 5.62 [t J = 8 Hz, 2H, CH_2 of chelate], 5.69 [t J = 8 Hz, 2H, CH_2 of chelate], 7.39 [m, 12H, aromatic CH], 7.74 [m, 16H, aromatic CH]. ^{13}C NMR ([D]chloroform, 20 °C): δ 70.9 [C_5H_3], 71.0 [C_5H_3], 76.5 [CH_2 of chelate], 76.6 [CH_2 of chelate], 76.8 [CH of chelate], 77.1 [CH of chelate], 80.4 [C_5H_3], 121.0, 121.4, 122.7, 123.0, 124.2, 125.8, 126.1, 126.7, 126.8, 131.1, 131.2, 131.3, 136.0, 136.5 [napthyl CH]. ^{11}B NMR ([D]chloroform, 20 °C): δ 32.4. IR (KBr disk, cm^{-1}): ν 2923 s, 1625 w, 1462 s, 1376 s, 1063 md, 855 w, 814 w, 722 md. UV/vis (chloroform): $\lambda_{max} = 461$ nm, $\epsilon = 347$ mol^{-1} cm^{-1} dm^3. MS (EI): M$^+$ = 970 (100%), exact mass (calcd) m/z 970.2909, (obs) 970.2908. 50% yield after recrystallization from hexanes (air-stable orange crystalline solid).

Spectroscopic Data for 1^{*s}. ^{1}H NMR ([D$_6$]benzene, 20 °C): δ 2.02 [s, 15H, Cp*], 4.03 [m, 1H, C_5H_4], 4.05 [m, 1H, C_5H_4], 4.45 [m, 1H, C_5H_4], 4.48 [m, 1H, C_5H_4], 5.43 [s, 2H, CH of chelate], 7.19−7.25 [m, 6H, C_6H_5], 7.42−7.45 [m, 4H, C_6H_5]. ^{13}C NMR ([D$_6$]benzene, 20 °C): δ 11.3 [CH_3 of Cp*], 71.2 [b, C_5H_4 quaternary], 76.0 (two overlapping signals), 76.7, 77.4 [CH of C_5H_4], 80.4 [Cp* quaternary], 86.6 [CH of chelate], 126.4, 127.2, 128.6 [aromatic CH], 140.2 [aromatic quaternary]. ^{11}B NMR ([D$_6$]benzene, 20 °C): δ 33.3. IR (KBr disk, cm^{-1}): ν 3423 md, 2962 md, 2904 md, 2854 w, 1636 w, 1496 md, 1479 st, 1451 md, 1382 st, 1325 md, 1315 md, 1301 md, 1261 w, 1208 w, 1174 w, 1125 st, 1027 st, 988 w, 818 w, 802 w, 762 w, 700 md, 686 w, 537 w, 482 w. UV/vis (chloroform): $\lambda_{max} = 445$ nm, $\epsilon = 193$ cm^{-1} mol^{-1} dm^3. MS(EI): M$^+$ = 478 (5%), exact mass (calcd) m/z 477.1797, (obs) 477.1791. 56% yield after recrystallization from hexanes (air-stable orange crystalline solid).

Spectroscopic Data for 2^{*s}. ^{1}H NMR ([D$_6$]benzene, 20 °C): δ 2.18 [s, 15H, Cp*], 4.77 [m, 1H, C_5H_3], 4.79 [m, 1H, C_5H_3], 5.33 [s, 1H, C_5H_3], 5.47 [s, 4H, CH of chelate], 7.23−7.32 [m, 12H, C_6H_5], 7.45−7.47 [m, 8H, C_6H_5]. ^{1}H NMR ([D]chloroform, 20 °C): δ 1.88 [s, 15H, Cp*], 4.27 [m, 1H, C_5H_3], 4.32 [m, 1H, C_5H_3], 4.55 [s, 1H, C_5H_3], 5.23 [s, 4H, CH of chelate], 7.27−7.34 [m, 20H, C_6H_5]. ^{13}C NMR ([D$_6$]benzene, 20 °C): δ 11.3 [CH_3 of Cp*], 65.9 [b, C_5H_4 quaternary], 80.7 [CH of C_5H_3], 80.9 [Cp* quaternary], 81.6, 83.7 [CH of C_5H_3] 86.6 [CH of chelate], 126.4, 128.6 [aromatic CH], 140.2 [aromatic quaternary]. ^{13}C NMR ([D]chloroform, 20 °C): δ 11.4 [CH_3 of Cp*], 65.7 [b, C_5H_4 quaternary], 80.5 [CH of C_5H_3], 81.2 [Cp* quaternary], 81.2, 83.3 [CH of C_5H_3], 86.5 [CH of chelate], 126.3, 128.4, 128.8 [aromatic CH], 139.7 [aromatic quaternary]. ^{11}B NMR ([D]chloroform, 20 °C): δ 32.7. IR (KBr disk, cm^{-1}): ν 3436 md, 3063 w, 3031 w, 2964 md, 2901 md, 1634 w, 1484 st, 1454 md, 1382 w, 1335 md, 1274 st, 1209 w, 1188 md, 1139 w, 1080 md, 1058 st, 1030 md, 985 md, 803 md, 760 md, 697 st, 650 w, 607 w, 534 w, 493 w. UV/vis (chloroform): $\lambda_{max} = 453$ nm, $\epsilon = 217$ cm^{-1} mol^{-1} dm^3. MS(EI): M$^+$ = 700 (5%), exact mass (calcd) m/z 698.2686, (obs) 698.2690. 58% yield after recrystallization from hexanes (air-stable orange crystalline solid).

Synthesis of 2^p. 2^p was synthesized from 1,1′-bis(dibromoboryl)ferrocene via route (ii) outlined in Scheme 1. Similar procedures were followed for the syntheses of 3^e and 4^e from 1′,3,3′-tris(dibromoboryl)ethylferrocene and 1,1′,3,3′-tetrakis(dibromoboryl)ferrocene, respectively, with the caveat that 3 or 4 equiv, respectively, of the diol reagent were employed for the syntheses of tris-, and tetrakis-functionalized ferroceneboronic esters. For these systems, route (ii), employing triethylamine (rather than n-butyllithium) as the base, was found to offer higher yields than route (i). To a solution of 1S,2S,3R,5S-2,3-pinanediol (0.65 g, 3.8 mmol) in a mixed toluene/THF solvent (40/20 cm^3) was added triethylamine (0.53 cm^3, 2.0 equiv) and a solution of 1,1′-bis(dibromoboryl)ferrocene (1.0 g, 0.5 equiv) also in toluene (30 cm^3). The reaction mixture was stirred for 24 h at room temperature, after which filtration, removal of the toluene solvent in vacuo, and recrystallization from hexanes at −30 °C yielded 2^p as an orange crystalline solid in 46% yield. Single crystals suitable for X-ray diffraction were obtained by slow cooling of a solution in hexanes.

Spectroscopic Data for 2^p. ^{1}H NMR ([D]chloroform, 20 °C): δ 0.83 [s, 6H, H-8], 1.25 [s, 6H, H-9], 1.28 [d J = 10 Hz, 2H, H-6a], 1.42 [s, 6H H-10], 1.89 [overlapping m, 4H, H-2, H-4a, H-5, H-7], 2.07 [t J = 5 Hz, 2H, H-1], 2.21 [m, 2H, H-6b], 2.35 [2H, m, H-4b], 4.32 [m, 4H, CH of C_5H_4], 4.34 [m, 2H, H-3], 4.35 [m, 2H, CH of C_5H_4], 4.37 [m, 2H, CH of C_5H_4]. ^{13}C NMR ([D]chloroform, 20 °C): δ 24.2, 26.7, 27.2, 29.1, 35.9, 38.3, 39.7, 51.4, 77.9, 85.8 [pinane backbone], 72.5, 72.6, 74.2, 74.3 [CH of C_5H_4]. ^{11}B NMR ([D]chloroform, 20 °C): δ 32.2. IR (KBr disk, cm^{-1}): ν = 3155 w, 2924 st, 2253 st, 1794 w, 1647 w, 1560 w, 1480 st, 1383 st, 1323 st, 1312 st, 1277 md, 1261 md, 1237 md, 1209 w, 1189 w, 1128 st, 1096 md, 1021 md, 916 st, 712 st. UV/vis (chloroform): $\lambda_{max} = 462$ nm, $\epsilon = 101$ cm^{-1} mol^{-1} dm^3. MS-(EI): M$^+$ = 542 (100%), exact mass (calcd) m/z 542.2457, (obs) 542.2456.

Spectroscopic Data for 3^e. ^{1}H NMR ([D]chloroform, 20 °C): δ 0.91 [t J = 7 Hz, 3H, CH_3 of Et], 2.26 [m, 2H, CH_2 of Et], 4.22 [m, 2H, C_5H_3], 4.24 [s, 1H, C_5H_3], 4.26 [b s, 12H, CH_2CH_2 of chelate], 4.45 [m, 1H, C_5H_3], 4.51 [m, 2H, C_5H_3]. ^{13}C NMR ([D]chloroform, 20 °C): δ 14.6, 21.7 [Et], 64.7 [CH_2 of chelate, 2 overlapping signals (ca. 2:1) at 64.72 and 64.46], 72.7, 74.3, 74.4, 78.4, 78.6, 81.7 [CH of C_5H_3]. ^{11}B NMR ([D]chloroform, 20 °C): δ 32.6 (b). IR (KBr disk, cm^{-1}): ν 2924 s, 1460 s, 1376 s, 1298 md, 1198 md, 1084 w, 1064 md, 991 md, 42 md, 850 w, 722 md, 686 w. UV/vis (chloroform): $\lambda_{max} = 454$ nm, $\epsilon = 199$ mol^{-1} cm^{-1} dm^3. MS (EI): M$^+$ = 424 (100%), exact mass (calcd) m/z 424.1118, (obs) 424.1119. 41% yield after recrystallization from hexanes (air-stable orange-yellow solid).

Spectroscopic Data for 4^e. ^{1}H NMR ([D]chloroform, 20 °C): δ 4.35 [s, 16H, CH of chelate], 4.53 [s, 4H, C_5H_3], 4.65 [s, 2H, C_5H_3]. ^{13}C NMR ([D]chloroform, 20 °C): δ 64.8 [chelate], 77.7, 80.8 [C_5H_3], quaternaries of C_5H_4 not observed. ^{11}B NMR ([D]chloroform, 20 °C): δ 32.3. IR (KBr disk, cm^{-1}): ν 3404 md, 1495 s, 1398 md, 1340 md, 1300 s, 1262 md, 1199 s, 1068 s, 992 md, 943 md, 860 w, 802 md, 691 md, 583 w, 500w. UV/vis (chloroform): $\lambda_{max} = 442$ nm, $\epsilon = 79$ mol^{-1} cm^{-1} dm^3. MS (EI): M$^+$ = 466 (100%), exact mass (calcd) m/z 466.1031, (obs) 466.1029. 31% yield after recrystallization from benzene (air-stable orange solid).

Alternative Syntheses from Ferroceneboronic Acids. Mono- and bis-boronic esters can also be synthesized by simple condensation chemistry utilizing the corresponding ferroceneboronic acid and diol, e.g., for 2^n, 1,1′-ferrocenediboronic acid (1.00 g, 3.66 mmol) and S-(2-napthyl)ethane-1,2-diol (1.38 g, 7.31 mmol) were dissolved in acetone in a sealed high-pressure tube. The mixture was stirred for 96 h at 75 °C, solvent removed in vacuo and the product purified by column chromatography (silica column, elution with chloroform). This method yielded samples of 2^n with identical spectroscopic properties to those synthesized from bis(dibromoboryl)ferrocene. The yield of 18% appears to be limited by the low solubility of 1,1′-ferrocenediboronic acid.

iii. Crystallographic Method. Data for $\mathbf{1^p}$, $\mathbf{2^p}$, $\mathbf{3^s}$, $\mathbf{4^s}$, $\mathbf{4^e}$, $\mathbf{4^p}$, $[\mathbf{1^s}]^+[CF_3SO_3]^-$, $[\mathbf{1^p}]^+[BF_4]^-$, and $[\mathbf{2^p}]^+[BF_4]^-$ were collected on an Bruker Nonius Kappa CCD diffractometer. Data collection and cell refinement were carried out using DENZO and COLLECT; structure solution and refinement used SIR-92, SHELXS-97, and SHELXL-97; absorption corrections were performed using SORTAV.[15] The quality of the data obtained for $\mathbf{4^p}$, while sufficient to confirm connectivity, precludes detailed discussion of structural data (the weakly diffracting nature of the crystals obtained precluding the collection of data beyond 23.6° in ϑ). This structure, together with those of the oxidation products $[\mathbf{1^s}]^+[CF_3SO_3]^-$, $[\mathbf{1^p}]^+[BF_4]^-$, and $[\mathbf{2^p}]^+[BF_4]^-$ is included in the Supporting Information only. For the remaining structures, details of data collection, structure solution, and refinement can be found in Table 1. Relevant bond lengths and angles are included in the figure captions, and complete details of each structure have been deposited with the CCDC (deposition numbers: 654486−654494). In addition, complete details for all structures (including CIFs) have been included in the Supporting Information.

iv. Electrochemical Method. Electrochemical analyses were carried out using the following conditions: electrolyte, 0.1 M $[^n\text{Bu}_4\text{N}][\text{PF}_6]$ in dichloromethane or acetonitrile; reference electrode standard, 0.1 M $[^n\text{Bu}_4\text{N}][\text{PF}_6]$, 0.01 M $AgNO_3$ in acetonitrile. Following degassing of the electrolyte solution with argon, background cyclic voltammetry (CV) scans were measured and a small sample (ca. 2−5 mg) of the ferroceneboronic ester was added to the solution. Further degassing served to purge the solution of any additional dissolved oxygen and agitate the solid Lewis acid to dissolve the compound, prior to spectral acquisition. Further CV scans were measured on the addition of excess solid $[^n\text{Bu}_4\text{N}]\text{F}\cdot x\text{H}_2\text{O}$ (or KF/18-crown-6), and on addition of ferrocene as a reference.

v. Kinetic Studies. In a typical experiment, an alicquot containing a known excess of tetra-*n*-butylammonium fluoride was added by syringe to 2.5 cm^3 of a stock solution of the boronic ester (17.5 mM) contained within the UV cell. The absorbance in the UV spectrum for the band at ca. 630 nm associated with the ferrocenium product was then recorded at 1 s intervals for a period of 2400 s (see figures for specific wavelengths associated with each ferrocenium species).

Results and Discussion

i. Synthetic and Structural Studies. Ferrocene-functionalized boronic esters of types **1**−**4** are readily synthesized in yields of 31−58% from the corresponding dibromoborylferrocene according to the routes outlined in Schemes 1−3. This simple substitution approach is applicable to a range of mono-, bis-, tris-, and tetrakis-borylated derivatives upon which a systematic investigation of sensor properties as a function of substitution pattern can be made (vide infra). While the ready availability of ferrocene derivatives bearing one, two, or four $-BBr_2$ groups via literature borylation protocols allows access to systems of types **1**, **2**, and **4** in two steps from ferrocene,[11] the synthesis of tris-borylated systems $\mathbf{3^s}$, $\mathbf{3^e}$, and $\mathbf{3^p}$ necessitates the use of ethylferrocene, from which 1′,3,3′-tris(dibromoboryl)ethylferrocene can readily be prepared.[12] In our hands, attempts to control the borylation of ferrocene itself with the aim of synthesizing the parent 1,3,1′-tris(dibromoboryl)ferrocene invariably result in the isolation of mixtures of polyborylated products.[11a] Pentamethylferrocene-based systems $\mathbf{1^{*s}}$ and $\mathbf{2^{*s}}$ are accessible in analogous fashion from 1′-(dibromoboryl)-1,2,3,4,5-pentamethylferrocene and 1′,3′-bis(dibromoboryl)-1,2,3,4,5-pentamethylferrocene, respectively. Primarily, *n*-butyllithium was employed as the base and was mixed with the diol in toluene or toluene/THF prior to the addition of the (dibromoboryl)-ferrocene; the use of triethylamine was also investigated, although separation of the triethylammonium bromide coproduct was typically less convenient. An alternative synthetic approach utilizing the direct condensation reaction between the diol and a ferroceneboronic acid could also be employed (e.g., for $\mathbf{2^n}$), although the lack of reliable, high-yielding routes to the tris- and tetrakis-boronic acids precludes this as a more general route.

Compounds **1**−**4** have been characterized by standard spectroscopic techniques and the structures of $\mathbf{1^p}$, $\mathbf{2^p}$, $\mathbf{3^s}$, $\mathbf{4^s}$, $\mathbf{4^e}$, and $\mathbf{4^p}$, as determined by single-crystal X-ray diffraction, are shown in Figures 2 and 3 (spectroscopic and crystallographic data for $\mathbf{1^s}$, $\mathbf{2^s}$, $\mathbf{1^e}$, and $\mathbf{2^e}$ have been reported previously).[8,10] From the perspective of fluoride binding studies, of particular note are the ^{11}B NMR shifts for the free Lewis acids which are in the range δ_B 30−34, typical of arylboronic esters; those of the corresponding fluoride adducts typically fall in the range δ_B 8−10.[16] In each case, the crystal structures confirm the planar three-coordinate geometry at boron implied by spectroscopic measurements, the angles at boron summing to 360° within the standard 3σ limit. In addition, the bending of the $-BX_2$ group out of the plane of the Cp ligand which is typically found for more Lewis acidic boryl groups appears to be a relatively minor effect for boronic esters [e.g., ∠Cp centroid−C(ipso)−B = 171.7−174.5° for $\mathbf{4^s}$ cf. 162.3° and 161.9° for (dibromoboryl)-ferrocene].[11b]

In the case of $\mathbf{4^s}$, NMR measurements at room temperature in toluene-d_8 are consistent with a more symmetrical structure than that of approximate (noncrystallographic) C_2 symmetry determined in the solid state. VT-NMR measurements, however, imply that rotation about the centroid−Fe−centroid axis (Figure 4) becomes slow on the NMR time scale at temperatures below −60 °C. Thus, for example, at −90 °C four distinct signals are observed for the methine protons of the boronic ester chelate rings, which coalesce at −60 °C before splitting into two singlet resonances which further sharpen on warming to room temperature. By simulating the experimental data, a barrier to rotation of $\Delta G^\ddagger = 13.0$ kcal mol^{-1} for the 'cogged' rotation of the η^5-$C_5H_3[B(OR)_2]_2]$ boronic ester units can be calculated, which compares with similar values of 11.0 and 13.1 kcal mol^{-1} for the analogous

---

[15] (a) DENZO: Otwinowski, Z.; Minor, W. *Methods in Enzymology*; Carter, C. W., Sweet, R. M., Eds.; Academic Press: New York, 1996; Vol. 276, p 307. (b) COLLECT: Data collection software, Nonius B.V., 1999. (c) SIR-92: Altomarte, A.; Cascarano, G.; Giocavazzo, C.; Guagliardi, A. *J. Appl. Crystallogr.* **1993**, *26*, 343. (d) Sheldrick, G.M. *SHELX97: Programs for Crystal Structure Analysis (Release 97-2)*; University of Göttingen: Göttingen, Germany, 1998. (e) SORTAV: Blessing, R. H. *Acta Crystallogr. A* **1995**, *51*, 33.

[16] Eaton, G. R.; Lipscomb, W. N. *NMR Studies of Boron Hydrides and Related Species*; Benjamin, New York, 1969.

Table 1. Crystallographic Data for **1**^{p}, **2**^{p}, **3**^{s}, **4**^{s}, and **4**^{e}

	1^p	**2**^{p}	**3**^{s}	**4**^{s}	**4**^{e}
empirical formula	$C_{20}H_{25}BFeO_2$	$C_{30}H_{40}B_2FeO_4$	$C_{54}H_{47}B_3FeO_6$	$C_{66}H_{54}B_4FeO_8$	$C_{18}H_{22}B_4FeO_8$
CCDC deposition no.	654487	654490	654491	654494	654492
fw	364.06	542.09	880.20	1074.18	465.45
temp (K)	150(2)	150(2)	150(2)	150(2)	150(2)
λ (Å)	0.71073	0.71073	0.71073	0.71073	0.71073
cryst syst	tetragonal	monoclinic	orthorhombic	orthorhombic	monoclinic
space group	$P4_2$	$P2_1$	$P2_12_12_1$	$C222_1$	$P2_1/n$
unit cell lengths *a*, *b*, *c* (Å)	16.805(2), 16.805(2), 6.327(1)	10.038(1), 7.408(1), 18.295(1)	9.2674(1), 15.9758(2), 30.0231(4)	12.358(1), 15.419(1), 29.757(1)	5.850(1), 9.863(1), 17.035(1)
α, β, γ (deg)	90, 90, 90	90, 92.14(1), 90	90, 90, 90	90, 90, 90	90, 96.89(1), 90
vol (Å^3), *Z*	1786.9(3), 4	1359.4(1), 2	4445.1(1), 4	5670.1(2), 4	975.6(1), 2
D_{calcd} (Mg/m^3)	1.353	1.324	1.315	1.258	1.584
abs coeff (mm^{-1})	0.852	0.589	0.392	0.322	0.819
F(000)	768	576	1840	2240	480
cryst size (mm^3)	0.25 × 0.22 × 0.20	0.28 × 0.25 × 0.08	0.50 × 0.38 × 0.17	0.40 × 0.38 × 0.35	0.38 × 0.25 × 0.10
θ range for data collection (deg)	3.64−26.36	2.96−27.48	3.62−26.37	3.57−26.37	3.57−26.36
index ranges (*h*, *k*, *l*)	−18 to 21, −16 to 20, −5 to 7	−13 to 12, −7 to 9, −23 to 23	−11 to 11, −19 to 19, −37 to 37	−12 to 15, −19 to 19, −37 to 37	−7 to 7, −12 to 12, −18 to 21
no. of reflns collected	5706	11 317	19 515	18 633	5048
no. of indep reflns/R_{int}	3179 (0.0735)	5346 (0.0740)	8873 (0.0829)	5619 (0.0956)	1987 (0.0599)
completeness to θ_{max} (%)	99.6	99.7	98.8	99.4	99.5
abs correction	semiempirical from equivs	semiempirical from equivs	semiempirical from equivs	semiempirical from equivs	semiempirical from equivs
max and min transmission	0.848 and 0.815	0.954 and 0.852	0.936 and 0.828	0.896 and 0.882	0.923 and 0.746
refinement method	full-matrix least-squares (F^2)	full-matrix least-squares (F^2)	full-matrix least-squares (F^2)	full-matrix least-squares (F^2)	full-matrix least-squares (F^2)
no. of data/restraints/params	3179/31/217	5346/1/340	8873/0/568	5619/0/357	1987/0/142
GOF on F^2	1.061	1.030	1.054	1.019	0.989
final *R* indices [$I > 2\sigma(I)$]	R1 = 0.0823, wR2 = 0.1793	R1 = 0.0559, wR2 = 0.1254	R1 = 0.0713, wR2 = 0.1594	R1 = 0.0513, wR2 = 0.1029	R1 = 0.0505, wR2 = 0.1278
R indices (all data)	R1 = 0.1338, wR2 = 0.2052	R1 = 0.0731, wR2 = 0.1349	R1 = 0.1110, wR2 = 0.1792	R1 = 0.0899, wR2 = 0.1178	R1 = 0.0689, wR2 = 0.1417
largest peak/hole (e Å^{-3})	1.083 and −0.605	0.457 and −0.474	1.220 and −0.612	0.375 and −0.368	0.577 and −0.795
absolute structure param	−0.06(6)	0.02(2)	−0.02(2)	0.01(2)	−

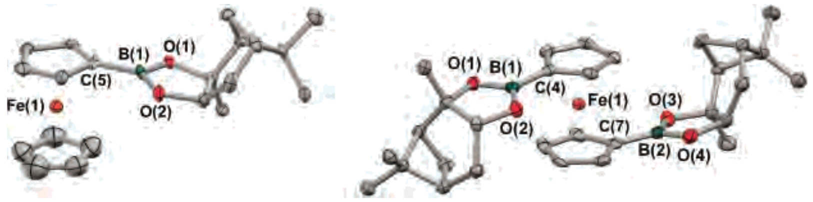

Figure 2. (left to right) Molecular structures of **1**^{p} and **2**^{p} with hydrogen atoms omitted for clarity and ORTEP ellipsoids set at the 50% probability level. Relevant bond lengths (Å) and angles (deg): (for **1**^{p}) B(1)−O(1) 1.368(11), B(1)−O(2) 1.342(11), B(1)−C(5) 1.550(11), Fe(1)−(η^5-C_5H_5) centroid 1.655(9), Fe(1)−(η^5-C_5H_4B) centroid 1.636(9), C(5)−B(1)−O(1) 123.5(8), C(5)−B(1)−O(2) 122.0(8), O(1)−B(1)−O(2) 114.5(8); (for **2**^{p}) B(1)−O(1) 1.364(5), B(1)−O(2) 1.377(6), B(1)−C(4) 1.538(6), B(2)−O(3) 1.362(6), B(2)−O(4) 1.372(7), B(2)−C(7) 1.540(7), Fe(1)−(η^5-C_5H_4B) centroid 1.646(5), 1.647(5), C(4)−B(1)−O(1) 123.1(4), C(4)−B(1)−O(2) 123.2(4), O(1)−B(1)−O(2) 113.8(4), C(7)−B(2)−O(3) 123.6(5), C(7)−B(2)−O(4) 122.3(4), O(3)−B(1)−O(4) 114.1(4).

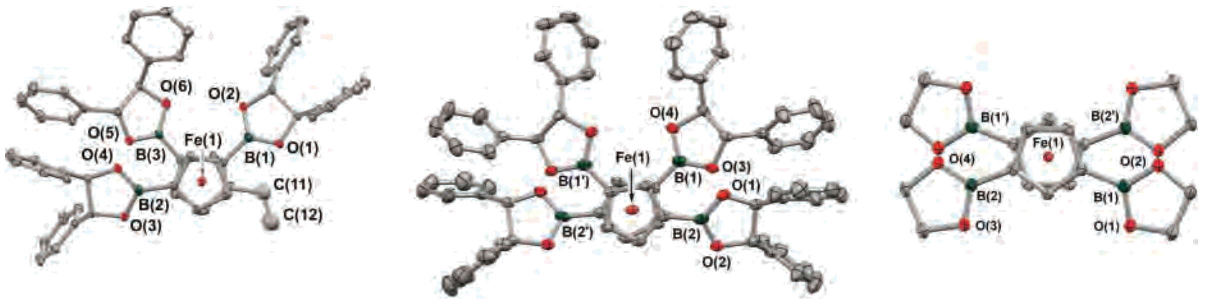

Figure 3. (left to right) Molecular structures of **3**^{s}, **4**^{s}, and **4**^{e} with hydrogen atoms omitted for clarity and ORTEP ellipsoids set at the 50% probability level. Relevant bond lengths (Å) and angles (deg): (for **3**^{s}) B(1)−O(1) 1.361(7), B(1)−O(2) 1.369(7), B(1)−C(5) 1.534(8), B(2)−O(3) 1.361(7), B(2)−O(4) 1.376(7), B(2)−C(3) 1.546(7), B(3)−O(5) 1.374(6), B(3)−O(6) 1.360(6), B(3)−C(7) 1.530(8), Fe(1)−(η^5-$C_5H_3B_2$) centroid 1.655(7), Fe(1)−(η^5-C_5H_3BC) centroid 1.671(7), C(5)−B(1)−O(1) 123.1(5), C(5)−B(1)−O(2) 123.7(5), O(1)−B(1)−O(2) 113.2(5), C(3)−B(2)−O(3) 123.9(5), C(3)−B(2)−O(4) 122.5(5), O(3)−B(1)−O(4) 113.6(4), C(7)−B(3)−O(5) 122.7(4), C(7)−B(3)−O(6) 123.5(4), O(5)−B(3)−O(6) 113.8(5); (for **4**^{s}) B(1)−O(3) 1.373(4), B(1)−O(4) 1.375(4), B(1)−C(3) 1.531(5), B(2)−O(1) 1.371(4), B(2)−O(2) 1.371(4), B(2)−C(6) 1.539(5), Fe(1)−(η^5-$C_5H_3B_2$) centroid 1.648(5), C(3)−B(1)−O(3) 124.1(3), C(3)−B(1)−O(4) 122.2(3), O(3)−B(1)−O(4) 113.6(3), C(6)−B(2)−O(1) 122.9(3), C(6)−B(2)−O(2) 124.0(3), O(1)−B(2)−O(2) 113.0(3), [symmetry transformations used to generate equivalent atoms (′): x, $-y + 2$, $-z + 2$]; (for **4**^{e}) B(1)−O(2) 1.362(4), B(1)−O(2) 1.3674), B(1)−C(1) 1.547(4), B(2)−O(3) 1.357(4), B(2)−O(4) 1.361(4), B(2)−C(4) 1.546(5), Fe(1)−(η^5-$C_5H_3B_2$) centroid 1.656(5), C(1)−B(1)−O(2) 120.8(3), C(1)−B(1)−O(2) 125.5(3), O(1)−B(1)−O(2) 113.6(3), C(4)−B(2)−O(3) 121.3(3), C(4)−B(2)−O(4) 125.0(3), O(3)−B(2)−O(4) 113.7(3), [symmetry transformations used to generate equivalent atoms (′): $-x$, $-y$, $-z$].

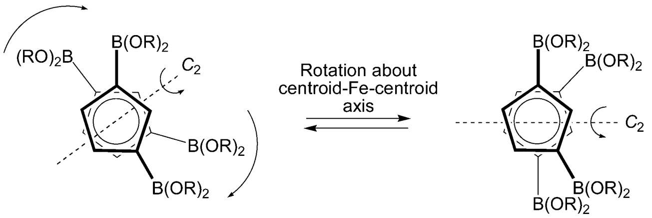

Figure 4. Fluxional interconversion of boronate ester groups by rotation of the 1,3-disubstituted cyclopentadienyl rings in **4**^{s} [$(OR)_2$ = R,R-OC(H)-PhC(H)PhO].

1,1′,3,3′-tetra(trimethylsilyl) and 1,1′,3,3′-tetra(*tert*-butyl)-ferrocenes.[17]

ii. Colorimetric Fluoride Ion Sensing: Thermodynamic Aspects. The monofunctional ferroceneboronic ester **1**^{s} can act as a selective receptor for fluoride in chloroform solution, with the binding event being accompanied by a cathodic shift of ca. −530 mV in the oxidation potential of the ferrocene center (from +131 to −403 mV with respect to ferrocenium/ferrocene).[10,18] Interaction of the boronic ester with the fluoride anion to give a four-coordinate adduct of the type $[FcB(OR)_2F]^-$ can be demonstrated explicitly by multinuclear (^1H, ^{11}B, and ^{19}F) NMR and electrospray mass spectrometry, with the relatively weak host/guest interaction (35.8 ± 9.8 M^{-1}) thought to be responsible for the high degree of selectivity for fluoride.[10] Despite the relatively large electrochemical shift on fluoride binding,[18] consistent with the conversion of a π-electron-withdrawing boronic ester to a strongly σ-electron-donating borate group,[5u,19] the thermodynamics of oxidation for $[\mathbf{1^s}\cdot F]^-$ ($E_{1/2}$ = −403 mV with respect to ferrocenium/ferrocene) are not sufficiently favorable such as to be effected by atmospheric oxygen.[20,21] In order to realize a sensor system based on the aerobic oxidation of the ferrocene backbone facilitated by fluoride coordination at boron, but which is capable of colorimetric (rather than simply electrochemical) detection, two possible strategies are conceivable, (i) multifunctional receptors which are capable of binding two or more equivalents of analyte and consequently bringing about a larger electrochemical shift on fluoride coordination and (ii) chemical modification

---

(17) (a) Luke, W. D.; Streitwieser, Jr., A. *J. Am. Chem. Soc.* **1981**, *103*, 3241. (b) Okuda, J.; Herdtweck, E. *J. Organomet. Chem.* **1989**, *373*, 99.

(18) Electrochemical shifts on fluoride ion binding are found to be strongly solvent dependent, e.g., for ferroceneboronic acid: $\Delta E_{1/2}$ = ca. 100 mV in water (ref 4a); $\Delta E_{1/2}$ = ca. −420 mV in dichloromethane.

(19) Carpenter, B. E.; Piers, W. E.; Parvez, M. E.; Yap, G. P. A.; Rettig, S. J. *Can. J. Chem.* **2001**, *79*, 857.

(20) The potential associated with the O_2/O_2^- couple in non-aqueous media is known to be strongly dependent on pH, e.g., for $O_2 + e^- \rightarrow O_2^-$, $E_{1/2}$ = −1000 mV versus ferrocenium/ferrocene in DMF, while for $O_2 + H^+ + e^- \rightarrow HO_2$, $E_{1/2}$ = −280 mV versus ferrocenium/ferrocene (also in DMF). For the oxidation of various fluoride adducts of borylated ferrocenes occurring in dichloromethane, the use of $[^nBu_4N]F\cdot xH_2O$ as the fluoride source inevitably introduces a protic component to the reaction mixture, thereby making O_2 a stronger oxidant than would be anticipated in strictly aprotic media. Sawyer, D. T.; Valentine, J. S. *Acc. Chem. Res.* **1981**, *14*, 393.

(21) Connelly, G.; Geiger, W. E. *Chem. Rev.* **1996**, *96*, 877.

Table 2. Electrochemical Data for **1**^{s}, **2**^{s}, **3**^{s}, **4**^{s}, **1**^{*s}, and **2**^{*s}

compound	peak−peak separation ($E_p^{ox} - E_p^{red}$) (mV)	$E_{1/2}$ relative to ferrocenium/ferrocene (mV)[a]
1^s	91[b]	+131[b]
	81[c]	+116[c]
2^s	70[b]	+206[b]
	80[c]	+222[c]
3^s	107[b]	+305[b]
4^s	90[b]	+430[b]
1^{*s}	81[b]	−169[b]
2^{*s}	80[b]	−83[b]

[a] Ferrocenium/ferrocene vs SCE: $E_{1/2} = 0.46$ (dichloromethane), 0.40 V (acetonitrile). [b] Dichloromethane solvent. [c] Acetonitrile solvent.

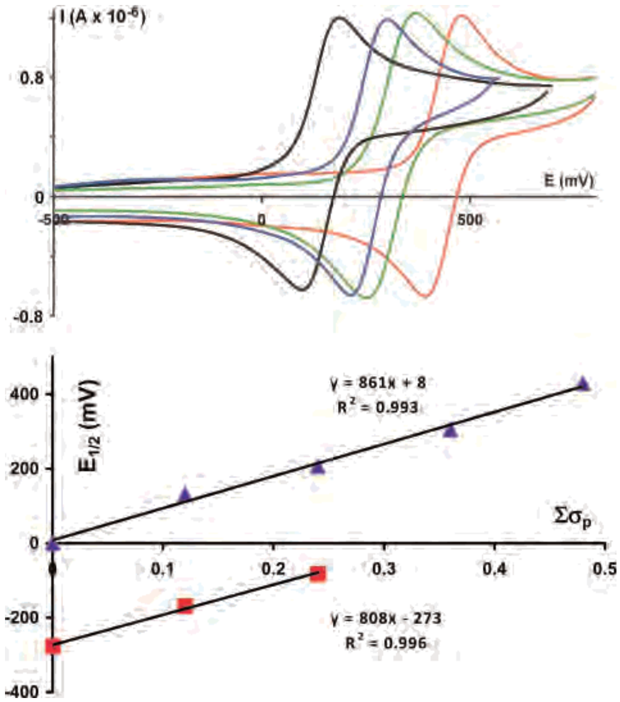

Figure 5. (upper) Cyclic voltammograms of **1**^{s} (black), **2**^{s} (blue), **3**^{s} (green), and **4**^{s} (red) in dichloromethane; **1**^{s}, **2**^{s}, and **4**^{s} referenced with respect to ferrocene/ferrocenium, **3**^{s} referenced with respect to ethylferrocene/ethylferrocenium. (lower) Plot of $E_{1/2}$ against the Hammett para parameter summed for each boronic ester substituent for **1**^{s}, **2**^{s}, **3**^{s}, **4**^{s} (blue triangles) and for **1**^{*s} and **2**^{*s} (red squares) [σ_p for B(OR)$_2$ is approximated by that for B(OH)$_2$, reported in ref 3a].

[e.g., by the inclusion of electron-donating substituents on the cyclopentadienyl ring(s)] such that the oxidation potentials of *both* the parent receptor *and* the resultant fluoride adduct are shifted cathodically by ca. −400 mV.

The first of these strategies has been examined by the synthesis of the related bis-, tris-, and tetrakis-boronic esters **2**^{s}, **3**^{s}, and **4**^{s}. In comparison with the monofunctional system (**1**^{s}), **2**^{s}, **3**^{s}, and **4**^{s} are characterized by oxidation potentials which are shifted *anodically*, consistent with the π-electron-withdrawing nature of the boronic ester group. A plot of $E_{1/2}$ vs $\Sigma\sigma_p$ (where σ_p is the Hammett para coefficient for the boronic acid substituent[22]) reveals a straight line plot (see Table 2 and Figure 5) and that the neutral molecule is stabilized with respect to the corresponding cation by ca. 110 mV per boronic ester substituent. This can be compared to a value of 120−160 mV per chloride substituent for the analogous chlorinated ferrocenes $C_{10}H_{10-x}Cl_xFe$.[23] Consistent with these observations, the *chemical* oxidation of ferroceneboronic esters of types **1**−**4** can readily be accomplished in dichloromethane by the use of a silver(I) oxidant [$E_{1/2}$(Ag$^+$/Ag) = +650 mV in dichloromethane],[21] while the corresponding reactions in acetonitrile do not appear to be feasible [$E_{1/2}$(Ag$^+$/Ag) = +40 mV in acetonitrile] (see Supporting Information for the crystal structures of [**1**^{s}]$^+$[CF$_3$SO$_3$]$^-$, [**1**^{p}]$^+$[BF$_4$]$^-$, and [**2**^{p}]$^+$[BF$_4$]$^-$).[21]

While these polyfunctional boronic esters are therefore thermodynamically more difficult to oxidize than **1**^{s}, the possibility of binding ≥2 equiv of fluoride offers the potential for significantly larger coordination-induced redox shifts. In practice, the success of this strategy can be gauged by the fact that **2**^{s}, **3**^{s}, and **4**^{s} all undergo irreversible orange-to-green color changes in chloroform solution in the presence of fluoride. This response is specific for fluoride (with no color change observed on addition of excess quantities of the ^{n}Bu$_4$N$^+$ salts of either Cl$^-$, Br$^-$, I$^-$, BF$_4^-$, PF$_6^-$, H$_2$PO$_4^-$, HSO$_4^-$, or NO$_3^-$) and, consistent with an oxidation process involving atmospheric oxygen, does not take place under strictly anaerobic conditions (vide infra). The mode of action of these receptors is best illustrated by **2**^{s}, for which a typical colorimetric response is shown in Scheme 4.

The binding of 2 equiv of fluoride (i.e., at both boron centers) for **2**^{s} can be demonstrated by a combination of ^{1}H, ^{11}B, and ^{19}F NMR spectroscopies,[8] and the ferrocene-to-ferrocenium oxidation process which accompanies fluoride binding is characterized in the UV/vis spectrum by the decay of bands at 341 and 449 nm with accompanying growth of features at 428 and 633 nm. The latter band is similar in energy and intensity to the feature at 617 nm in the spectrum of ferrocenium itself, and which has been attributed to a $^2E_{2g} \rightarrow {}^2E_{1u}$ charge-transfer process.[24] While these data are strongly suggestive of the colorimetric response being associated with the formation of a ferrocenium ion, the electrochemical processes involved can be probed more deeply by CV. Thus, while **2**^{s} itself undergoes a one-electron oxidation at +206 mV with respect to ferrocenium/ferrocene (cf. +131 mV for **1**^{s}), two waves are observed in the cyclic voltammogram in the presence of excess fluoride (see Supporting Information). These are measured at −384 and −746 mV (with respect to ferrocenium/ferrocene) and represent net shifts of −590 and −960 mV compared to **2**^{s} itself. While the former shift is very similar to that measured for **1**^{s} with/without fluoride (−530 mV) and is therefore assigned to the oxidation of the mono(fluoride) adduct [**2**^{s}·F]$^-$, the larger shift (and the fact that **2**^{s} is oxidized in air in the presence of excess fluoride) is strongly suggestive of the formation of the bis(fluoride) adduct [**2**^{s}·2F]$^{2-}$. The electrochemical potential associated with this 1:2 adduct (unlike those associated with the 1:1 adducts [**1**^{s}·F]$^-$ and [**2**^{s}·F]$^-$) is then likely to be consistent with oxidation by the O$_2$/O$_2^-$ couple.[20] Furthermore, the approximate additivity of

---

[22] Hansch, C.; Leo, A.; Taft, R. W. *Chem. Rev.* **1991**, *91*, 165.

[23] Brown, K. N.; Gulyas, P. T.; Lay, P. A.; McAlpine, N. S.; Masters, A. F. *J. Chem. Soc., Dalton Trans.* **1993**, 835.

[24] Lever, A. B. P. *Inorganic Electronic Spectroscopy*, 2nd ed.; Elsevier: Amsterdam, 1984; pp 659−671.

Scheme 4 Color Change and Chemical Mode of Action for **2**^{s} as a Colorimetric Fluoride Ion Sensor in Chloroform Solution[a]

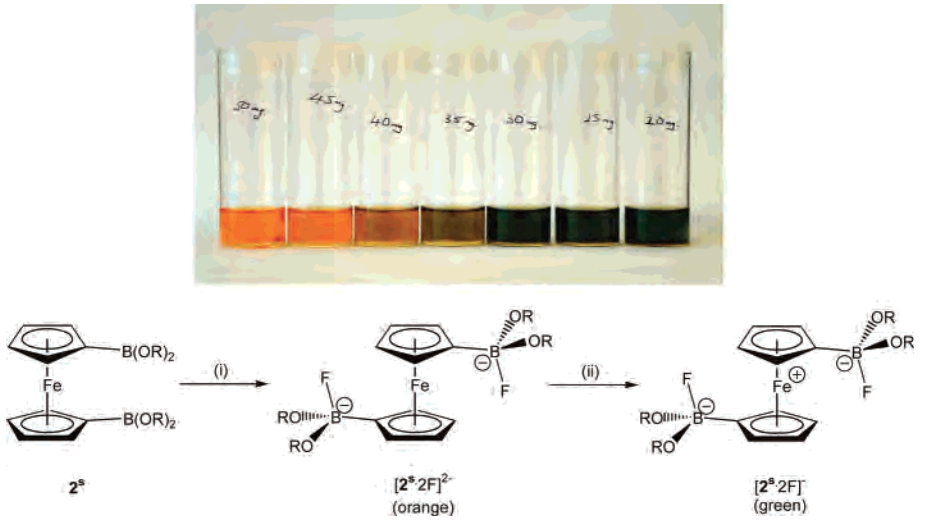

[a] Reagents and conditions: (i) fluoride source ([^{n}Bu$_4$N]F or KF/18-crown-6); (ii) aerobic oxidation.

the redox shifts measured for **2**^{s} is consistent with the successive conversion of one and two boronic esters to anionic boronate substituents.[19] Tris- and tetrakis-functionalized analogues **3**^{s} and **4**^{s} undergo similar orange-to-green color changes on exposure to fluoride in air, although with vastly differing kinetics compared to **2**^{s} (vide infra). Cyclic voltammograms of **3**^{s} and **4**^{s} in the presence of excess fluoride are typically indicative of irreversible electrochemical processes, and detailed analysis is precluded. However, the magnitudes of the redox shifts implied by the observed aerobic oxidation of **3**^{s} and **4**^{s} in the presence of fluoride strongly suggest the binding of two or more equivalents of the anion in each case. Subsequent mass spectrometric and kinetic measurements (vide infra) have been shown to be consistent with the species undergoing oxidation being the bis(fluoride adduct) i.e., [**3**^{s}·2F]$^{2-}$ or [**4**^{s}·2F]$^{2-}$.

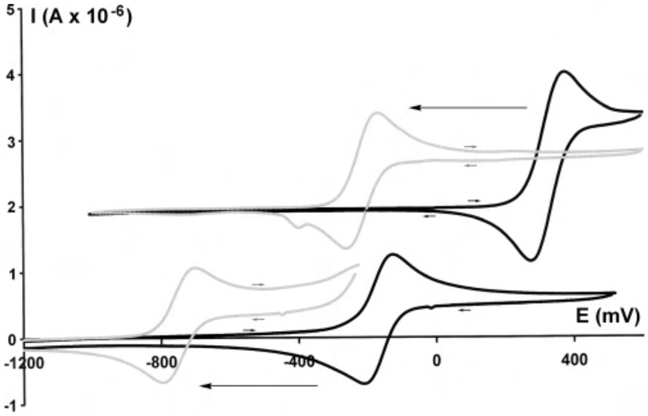

Figure 6. (upper) Cyclic voltammogram for **1**^{s} in dichloromethane (black trace) and in the presence of fluoride (gray trace). (lower) Analogous voltammograms for **1**^{*s} (all spectra referenced with respect to ferrocene/ferrocenium).

Given that permethylation of one of the Cp rings of ferrocene is reported to lead to a ca. −300 mV cathodic shift in the oxidation potential,[25] a suitable chemical modification which might lead to the realization of strategy (ii) involves the use of the pentamethylferrocene analogue of **1**^{s}, i.e., **1**^{*s}. In practice, **1**^{*s} is readily synthesized in two steps from pentamethylferrocene (Scheme 3) and displays the expected shift in redox potential (ca. −300 mV) compared to the parent system **1**^{s}. Thus in dichloromethane solution, **1**^{*s} is oxidized at −169 mV (with respect to ferrocenium/ferrocene), compared to +131 mV for **1**^{s}. On addition of fluoride (as [^{n}Bu$_4$N]F·xH$_2$O), the oxidation potentials of *both* **1**^{s} and **1**^{*s} undergo similar shifts (−530 and −580 mV, respectively; Figure 6). The net electron-donating effect of permethylation of one of the Cp rings, therefore, is to shift the oxidation potentials of both **1**^{*s} and [**1**^{*s}·F]$^{-}$ cathodically by between −300 and −400 mV. As such, [**1**^{*s}·F]$^{-}$ undergoes aerobic oxidation, and **1**^{*s} therefore acts as a colorimetric (orange to green) fluoride sensor. A potential advantage conferred by this latter strategy, as opposed to that offered by the polyfunctional systems **2**^{s}, **3**^{s}, and **4**^{s}, is that 1 rather than 2 equiv of analyte are required.

iii. Colorimetric Fluoride Ion Sensing: Kinetic Aspects. A key goal of the current program is a fuller understanding of the influence of receptor/system design on the *rate* of response. In particular, we were keen to probe methods of controlling oxidation kinetics based on synthetically facile chemical modification of the parent ferroceneboronic ester. Thus, the effects of altering the number of boronic ester binding sites (e.g., via systems of types **1**, **2**, **3**, and **4**), the ancillary cyclopentadienyl substitution pattern (via **1**^{*s} and **2**^{*s}) and more subtly by varying the boronic ester substituents themselves (e.g., via **4**^{s}, **4**^{p}, and **4**^{n}) have all been probed. Typically, the kinetics of the colorimetric response were assayed by UV/vis spectroscopy, the intensity of the band at ca. 630 nm associated with the ferrocenium product being monitored as a function of time. These studies also highlight the key role of the oxidant (in addition to the receptor) in determining the kinetics of response. Thus, in the absence of dissolved dioxygen (i.e., under strictly anaerobic conditions) a solution of **4**^{s} in chloroform shows no colorimetric response to the addition of [^{n}Bu$_4$N]F, and the band at

---

(25) Noviandri, I.; Brown, K. N.; Fleming, D. S.; Gulyas, P. T.; Lay, P. A.; Masters, A. F.; Phillips, L. *J. Phys. Chem. B* **1999**, *103*, 6713.

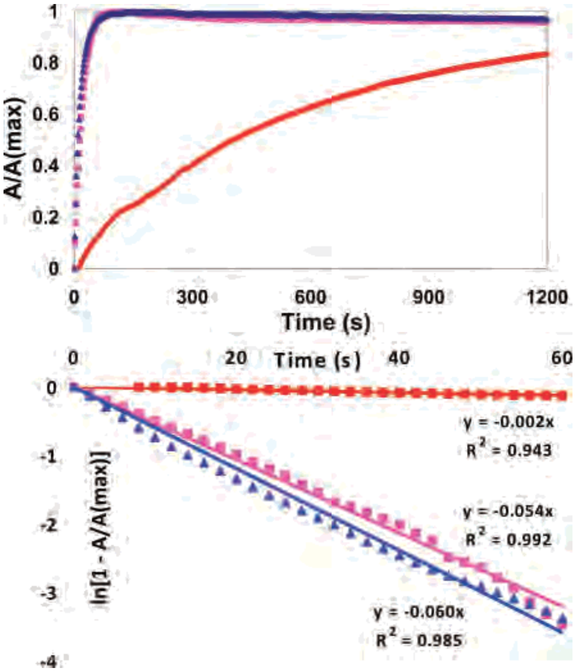

Figure 7. (upper) Plot of normalized absorbance against time for the band at ca. 630 nm associated with the oxidized ferrocenium species formed on addition of [^{n}Bu$_4$N]F (15 equiv) to the stilbene diolate-functionalized receptors **2**^{s}, **3**^{s}, and **4**^{s} (17.5 mM). Red, **2**^{s} (monitored at 633 nm); pink, **3**^{s} (654 nm); blue, **4**^{s} (640 nm). (lower) Logarithmic plot to determine pseudo-first-order rate constants. Red, **2**^{s}; pink, **3**^{s}; blue, **4**^{s}.

640 nm due to the oxidized ferrocenium product is absent. Reactions carried out in bench chloroform or in chloroform presaturated with dioxygen, on the other hand, undergo aerobic oxidation with mutually similar absorption/time profiles, while solutions presaturated with argon—but exposed to air on addition of the fluoride source—are characterized by an initial rate (ν_i) which is reduced by ~70% (see Supporting Information). Presumably, in the latter case, the sensor response is limited by the rate of diffusion of dioxygen into solution; this factor is found to be particularly important for the fabrication of *solid state* sensor devices incorporating **4**^{s} and related receptors, where the incorporation of a suitable redox-matched solid-state oxidant is required in order to facilitate a usable colorimetric response over a realistic time frame.[9]

UV/vis monitoring of the bands associated with the respective ferrocenium products is consistent with significant variation in reaction kinetics as a function of the number of boronic ester binding sites. Thus, plots of normalized absorbance, *A*/*A*(max), against time for each of **2**^{s}, **3**^{s}, and **4**^{s} (Figure 7) under standardized conditions (15 equiv of fluoride, bench chloroform, 20 °C) are consistent with a marked enhancement of the rate of formation of the ferrocenium product for the tris- and tetrakis-functionalized products, compared to **2**^{s}. Assuming pseudo-first-order kinetics [given the large excess of fluoride used and the knowledge that, under such solvent conditions, the rate is not oxidant limited (vide supra)], the linear plots reproduced in Figure 7 yield similar rate constants for **3**^{s} and **4**^{s} (5.4×10^{-2} and 6.0×10^{-2} s^{-1}, respectively) which are at least an order of magnitude greater than the analogous parameter associated with **2**^{s} (2×10^{-3} s^{-1}).

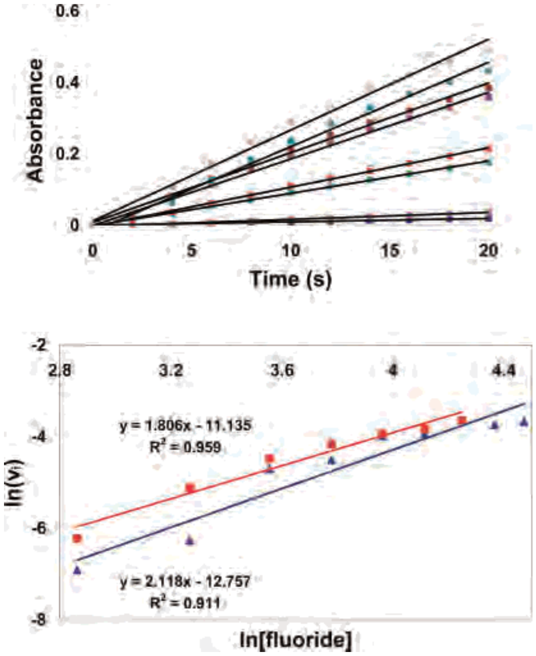

Figure 8. (upper) Plot of absorbance against time for the growth of the band at 654 nm associated with the ferrocenium species formed on oxidation of **3**^{s} (17.5 mM) in the presence of different concentrations of [^{n}Bu$_4$N]F. The eight traces (bottom to top) were obtained for [^{n}Bu$_4$N]F concentrations of 17.5, 26.3, 35.0, 43.8, 52.5, 61.3, 78.8, and 87.5 mM, and initial rates (ν_i) obtained by fitting the data to a linear expression in time. (lower) Plot of ln(ν_i) against ln(fluoride concentration) for the generation of the ferrocenium species formed on oxidation of **3**^{s} in the presence of different concentrations of [^{n}Bu$_4$N]F. Two independent sets of data are plotted, represented by the blue triangles corresponding to the kinetic runs described by the upper figure.

In order to probe potential factors underlying these observations, the kinetics of the reactions of **3**^{s} and **4**^{s} with fluoride were further probed as a function of fluoride concentration. The results of these studies are shown in Figures 8 and 9. In each case, the intensity of the absorption characteristic of the ferrocenium product (at 654 and 640 nm for **3**^{s} and **4**^{s}, respectively) was measured as a function of time for a series of kinetic runs in which the fluoride concentration was systematically varied. Estimates of the initial rate (ν_i) for each run were then obtained by fitting a linear function to the absorbance/time data for $t \leq 20$ s. Using the method of initial rates,[26] the order of the reaction with respect to fluoride was then obtained from the gradient of the linear plot of ln(ν_i) against ln[F$^-$]. The results of two such series of experiments (for both **3**^{s} and **4**^{s}) are shown in Figures 8 and 9, respectively. For each compound, the data is consistent with a mechanism in which *2* equiv of fluoride are bound by the polyfunctional Lewis acid, prior to aerobic oxidation. Such results are consistent with electrochemical studies (vide supra) which show that the conversion of (at least) two electron-withdrawing boronic ester groups to electron-donating boronates is required to generate a ferrocene which is sufficiently electron rich to be oxidized by dioxygen.

Electron-transfer processes involving ferrocene and inorganic oxidants typically proceed via outer-sphere mecha-

---

[26] Laidler, K. J. *Chemical Kinetics*; Harper and Row: New York, 1987; Chapter 2.

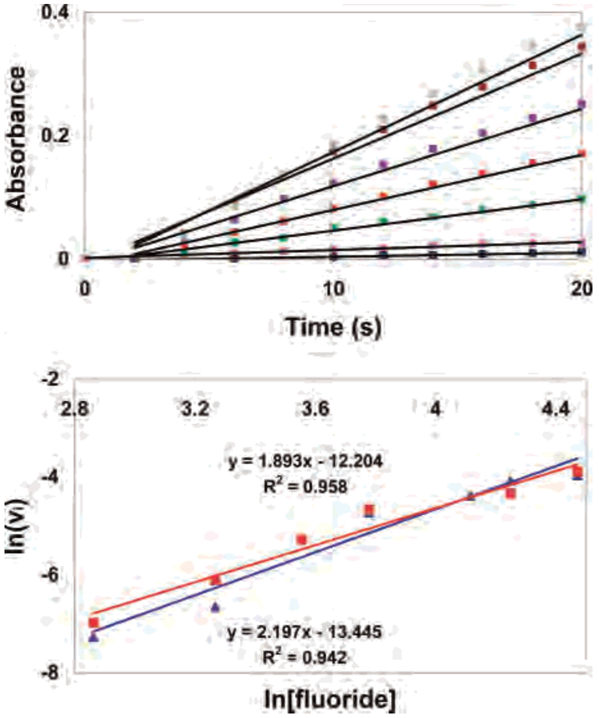

Figure 9. (upper) Plot of absorbance against time for the growth of the band at 640 nm associated with the ferrocenium species formed on oxidation of **4**^{s} (17.5 mM) in the presence of different concentrations of $[^{n}\mathrm{Bu}_4\mathrm{N}]\mathrm{F}$. The seven traces (top to bottom) were obtained for $[^{n}\mathrm{Bu}_4\mathrm{N}]\mathrm{F}$ concentrations of 17.5, 26.3, 35.0, 43.8, 61.3, 70, and 87.5 mol dm^{-3}, and initial rates (ν_i) obtained by fitting the data to a linear expression in time. (lower) Plot of ln(ν_i) against ln(fluoride concentration) for the generation of the ferrocenium species formed on oxidation of **4**^{s} in the presence of different concentrations of $[^{n}\mathrm{Bu}_4\mathrm{N}]\mathrm{F}$. Two independent sets of data are plotted, represented by the blue triangles corresponding to the kinetic runs described by the upper figure.

nisms, with the increased rates of transfer, e.g., for methylated ferrocenes (vs ferrocene itself) reflecting Marcus theory and the more favorable thermodynamics of oxidation.[27] Consistent with this, the rate of oxidation of **2**^{*s} in the presence of fluoride is ca. double that measured for **2**^{s} (see Supporting Information). In the cases of **2**^{s}, **3**^{s}, and **4**^{s}, the rates of oxidation (in the presence of fluoride) do not appear on first inspection to be governed by similar factors, since the *thermodynamics* of oxidation for $[\mathbf{3}^{s}{\cdot}2\mathrm{F}]^{2-}$ and $[\mathbf{4}^{s}{\cdot}2\mathrm{F}]^{2-}$, which feature one and two pendant (π-electron-withdrawing) boronic ester groups, respectively, would be expected to be less favorable than that for $[\mathbf{2}^{s}{\cdot}2\mathrm{F}]^{2-}$. On the other hand, it is possible that the remaining (uncomplexed) three-coordinate boron center(s) in $[\mathbf{3}^{s}{\cdot}2\mathrm{F}]^{2-}$ and $[\mathbf{4}^{s}{\cdot}2\mathrm{F}]^{2-}$ offer(s) a facile route for electron transfer from the electron-rich ferrocene to the oxidant.[28] It is also possible that electron transfer is mediated via the π system of aromatic substituents pendant to the boronic ester chelate ring. Thus, while **4**^{s} and **4**^{n}, featuring phenyl and napthyl substituents, respectively, display remarkably similar oxidation kinetics, **4**^{p} (which contains the saturated pinane substituent) is oxidized ca. five times slower (see Supporting Information). Alternatively, it is possible that the pendant boronic ester groups present in **3**^{s} and **4**^{s} offer a mechanism for fluoride chelation in the oxidized (and therefore more Lewis acidic) ferrocenium products, which could influence the overall oxidation thermodynamics and hence the Marcus-predicted rate.

Conclusions

The thermodynamic factors underlying the potential use of ferroceneboronic esters as electrochemical or colorimetric fluoride ion sensors have been determined. Thus, if the shift in electrochemical potential associated with the conversion of one (or more) boronic ester group(s) to anionic boronate(s) is sufficient to allow oxidation of the resulting receptor/analyte complex by dioxygen, colorimetric sensing is possible. In practice, from a prototype monofunctional system **1**^{s}, which displays selectivity in fluoride binding, but an insufficient electrochemical shift, two chemical modification strategies have been shown to be successful in designing a colorimetric sensor—namely the use of the more strongly electron-donating Cp* ancillary ligand—or receptors featuring two or more binding sites. In the case of **2**^{s}, the binding of 2 equiv of fluoride gives an electrochemical shift (in chloroform) which is approximately double that for **1**^{s}. Tris- and tetrakis-functionalized systems **3**^{s} and **4**^{s} are also shown to be oxidized as the bis(fluoride) adducts, presumably because of fast oxidation kinetics, relative to the rate of the (electrostatically unfavorable) binding of a third equivalent of fluoride. Furthermore, the rate of sensor response (as measured by UV/vis spectroscopy) is found not only to be dependent on the availability of oxidant (both in solution and in the solid state) but also to be enhanced by pendant (uncomplexed) three-coordinate boronic ester functions and/or delocalized aromatic substituents.

Acknowledgment. The financial support of the EPSRC and the Joint Grants Scheme is gratefully acknowledged, as are the efforts of the EPSRC National Mass Spectrometry Service Centre, Swansea.

Supporting Information Available: Complete details of all crystal structures (including CIFs); CV of **2**^{s} with/without fluoride; kinetic data obtained from UV/vis monitoring of oxidation chemistry as a function of (i) solvent oxygenation, (ii) boronic ester backbone, and (iii) ancillary ligand set. This material is available free of charge via the Internet at http://pubs.acs.org.

IC701494P

---

(27) For earlier studies on the kinetics of reduction of dioxygen by ferrocene derivatives, see for example: Fukuzumi, S.; Mochizuki, S.; Tanaka, T. *Inorg. Chem.* **1989**, *28*, 2459.

(28) For reviews detailing electronic interaction via three-coordinate boron, see for example: (a) Elschenbroich, C.; Wolf, M.; Burghaus O.; Harms, K.; Pebler, J. *Eur. J. Inorg. Chem.* **1999**, 2173. (b) Entwistle, C. D.; Marder, T. B. *Angew. Chem., Int. Ed.* **2002**, *42*, 2927. (c) Weber, L.; Domke, I.; Schmidt, C.; Braun, T.; Stammler, H.-G.; Neumann, B. *Dalton Trans.* **2006**, 2127. (d) Sundararaman, A.; Venkatasubbaiah, K.; Victor, M.; Zakharov, L. N.; Rheingold, A. L.; Jäkle, F. *J. Am. Chem. Soc.* **2006**, *128*, 16554.